Head Disk Interface Response during Operational Shock with Disk-Ramp Contact

Liping Li and David B. Bogy

Computer Mechanics Laboratory

Department of Mechanical Engineering

University of California

Berkeley, CA 94720

Abstract

In hard disk drives (HDD) the ramp load/unload (LUL) technology has proved to be a better alternative to the contact start-stop (CSS) approach due to the advantages of increasing areal density and greater durability. However, the application of the LUL ramps in HDDs introduces the possibility of collisions between the disk and the ramps since the ramps must slightly overlap the disk's outer radius. Therefore, it is important to study the ramp effects on the HDD's response during a shock. A reduced model of a deformable ramp is developed and implemented into a multi-body operational shock (op-shock) model. Numerical analyses using three different ramp models (no-ramp, rigid ramp and deformable ramp) are carried out to study the HDD's failure dependence on the different ramp models.

1. INTRODUCTION

The ramp LUL technology in HDDs was introduced in the mid-1990s as a better alternative to contact CSS [1]. In the CSS method, the sliders, which carry the read-write

transducers, rest on a laser textured landing zone at the disk's inner radius surface when the power is off, and they stay remain the disk until the power is turned on and an air bearing is established to create a clearance. There are several limitations for the CSS method, such as serious wear problems, less usage of disk media surface for data, etc. The ramp LUL technology has proved to be a historic breakthrough because of the advantages of increasing the disk storage areal density, greater durability, more efficient power utilization and superior non-operational shock resistance. In this method, the slider is lifted off the disk and parked on the ramp which sits near the outer radius of the disk (Fig.1) when the power is off. During a powering-on process, the slider is moved off the ramp and over the disk surface to establish its air bearing after the disk reaches an appropriate spinning speed. Most of the current commercial mobile drives apply the LUL ramp technology.

However, the application of the LUL ramp in HDDs introduces the possibility of collision between the disk and ramp during a shock while the HDD is operational (op-shock) as the ramp overlaps the outer edge of the disk with a small clearance. So it is important to study the ramp effects on the head disk interface (HDI) response during an op-shock event. Various experimental and simulation studies [2-14] have been carried out in the past to investigate the shock response of the mechanical system and the HDI. However, the deformable LUL ramp was not implemented in the prior models. Rai and Bogy [15, 16] proposed a method in which both the structural components and the air bearing were modeled in detail and were coupled with each other. However, in their research the ramp was modeled as a rigid body (Fig.2) that was fixed; hence the effects due to the flexibility of the ramp were not considered in their work.

In this investigation, a deformable ramp model is developed, and the ramp constraint is implemented into a multi-body op-shock model [17]. Numerical analyses using three different ramp models (no-ramp, rigid ramp and deformable ramp) are carried out to study the ramp effects on the HDI response.

2. SYSTEM MODELING

The HDI in a mobile drive consists of a slider and a spinning disk, which are coupled through an air bearing. Hence the stability of the HDI depends on the dynamic responses of the air bearing and structural components, including the suspension. In this study the model consists of a slider-disk pair, a suspension which has the slider attached and a deformable LUL ramp which is located at the outer edge of the disk. The ramp model is created in the commercial FE software ANSYS and is shown in Fig.3.

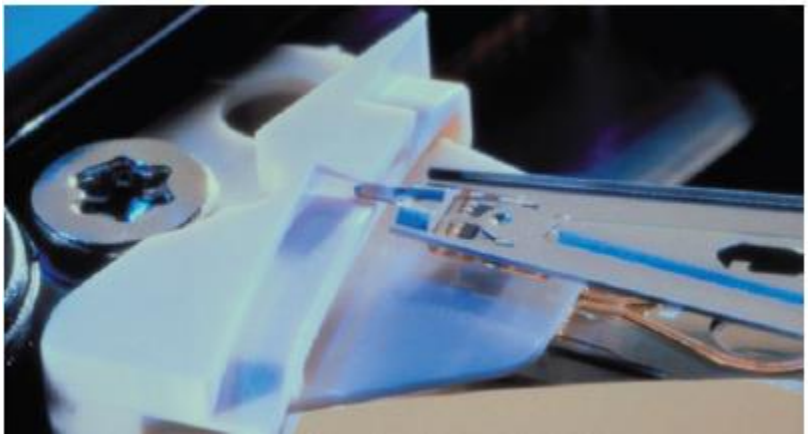

Fig.1 A slider parking on the ramp [1]

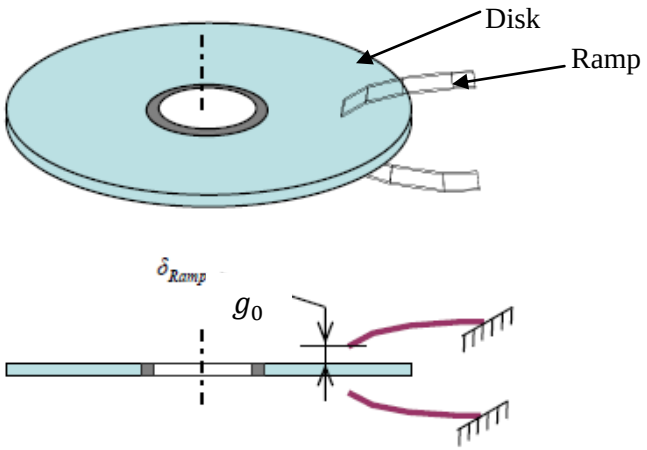

Fig.2 Idealized rigid ramp model; g_0 is the clearance between the ramp and disk.

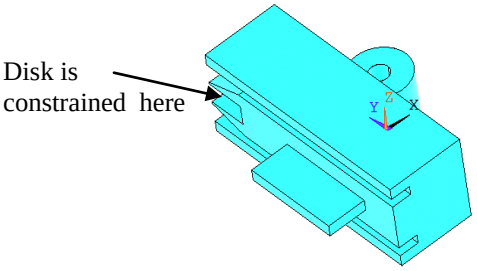

Fig.3 More realistic deformable deformable ramp model

The constraint imposed by the ramp on the spinning disk can be expressed as:

$$\left|w_{disk}(r_{ramp}, \theta_{ramp})\right| \leq \left|w_{ramp}\right| + g_0 \tag{1}$$

where g_0 is the minimum designed static clearance between the disk and the ramp, chosen to be 100 μm in this investigation. w_{disk} is the disk's transverse displacement at the ramp position, which is determined by the radius r_{ramp} and angular coordinate θ_{ramp}. w_{ramp} is the ramp displacement, which is equal to zero in the rigid ramp model but has a solution determined value in the deformable case.

So the ramp constraint can be written as:

$$[Q]\{u\} = \{g_0\}. \tag{2}$$

For the top ramp, $[\mathrm{Q}] = [1 \quad -1]$, $\{\mathrm{u}\} = \begin{Bmatrix} \mathrm{w_{disk}} \\ \mathrm{w_{t\_ramp}} \end{Bmatrix}$; while for the bottom ramp, $[\mathrm{Q}] = [-1 \quad 1]$, $\{\mathrm{u}\} = \begin{Bmatrix} \mathrm{w_{disk}} \\ \mathrm{w_{b\_ramp}} \end{Bmatrix}$. $\mathrm{w_{t\_ramp}}$ and $\mathrm{w_{b\_ramp}}$ are the top and bottom ramp displacements, respectively.

The disk-ramp contact is simplified as a point-to-point contact, so a Lagrange multiplier method is used to model the ramp's constraint of the disk's displacement. Then the dynamic equation of motion can be written as:

$$\begin{cases} [\mathrm{M}]\{\ddot{\mathrm{u}}\} + [\mathrm{C}]\{\dot{\mathrm{u}}\} + [\mathrm{K}]\{\mathrm{u}\} + [\mathrm{Q}]^{\mathrm{T}}\{\lambda\} = \{\mathrm{F}\} \\ [\mathrm{Q}]\{\mathrm{u}\} = \{\mathrm{g_0}\} \end{cases}, \tag{4.3}$$

where λ is the reaction force arising due to the ramp constraint. $[M]$, $[C]$ and $[K]$ are the mass, damping, and stiffness matrices for the structural system. $\{F\}$ is the external force. $\{\mathrm{u}\}$ is the structural displacement.

3. SIMULATION PROCEDURE

The fluid-structure interaction problem is solved to find the slider's flying height (FH). In this simulation, the air bearing force on the spinning disk is negligible in comparison to the inertia force. However, the disk's deformation affects the air bearing slider's response. So it is a one-way coupling problem. The simulation starts with an initial guess of the slider's relative flying attitude (FH, pitch and roll). After the air bearing problem is solved, the pressure distribution under the slider is evaluated and the resultant forces are calculated. The air bearing force, together with other interfacial forces, are applied to the structure as an external force. The structure's displacement is then solved to get a new flying attitude. The fixed-point iteration is carried out until the slider's displacement converges at each time step.

4. RESULTS AND ANALYSIS

In this analysis a shock is modeled as a half sinusoid acceleration wave in the axial direction that is defined by its amplitude and its pulse width (shown in Fig.4). A positive shock is defined as one that causes the disk to initially move towards the slider, while in a negative shock, the disk initially moves away from the slider. The minimum clearance between the slider and the disk surface (h_{min}) is used as the failure criterion. When h_{min} becomes less than zero, head-disk contact occurs and the HDI is 'failed'. This investigation is carried out for a 2.5'' form factor HDD.

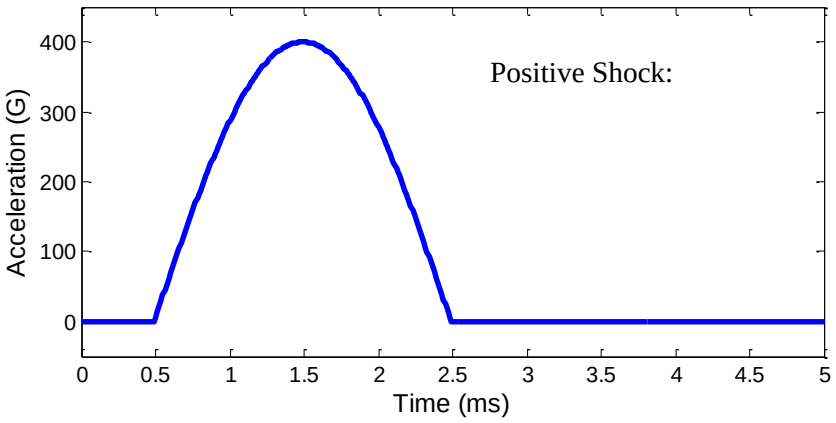

Fig.4 Operational shock acceleration wave form in the z-direction

4.1 Three Ramp Model Results for Shocks with a Pulse Width of 2.0 ms

In this section we investigate a positive shock with amplitude of 400G and pulse width of 2.0 ms to study the HDI responses for three ramp cases: the no-ramp, rigid ramp and deformable ramp models. Fig.5 shows the disk's absolute displacement as a function of time at the slider's center position for the three cases. Fig.5(1) shows that for no-ramp the disk moves smoothly during the simulation time, and no disk-ramp contact force is shown in Fig.6(1). In contrast, the disk's displacement in the rigid ramp case (Fig.6(2)) shows that the disk could not move upwards any more after 1 ms, when the maximum disk's

displacement at the slider's center is about 50 μm. The reason is that the slider is flying at the mid-radius of the disk and the disk's outer radius displacement is limited by the ramp to about 100 μm. Fig.6(2) confirms that the disk contacts the ramp at 1 ms. For the deformable ramp model, it is also found that the disk contacts the top ramp at about 1 ms as can be seen in Fig.6(3). However, the disk continues to move upwards almost as in the no-ramp case even after contact with the top ramp (Fig.5(3)). Moreover, the disk moves smoothly during the simulation period, which is different from the rigid ramp case.

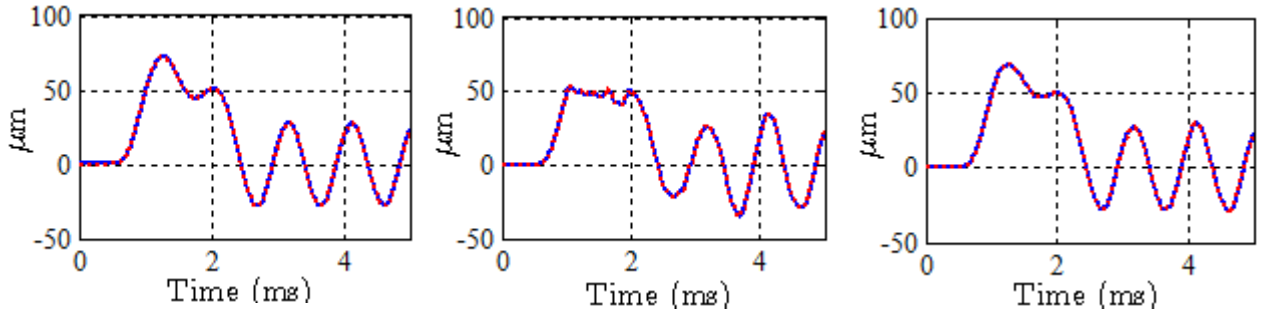

(1) (2) (3)

Fig.5 Disk absolute displacement at slider center position: (1) no ramp model; (2) rigid ramp model; (3) deformable ramp model.

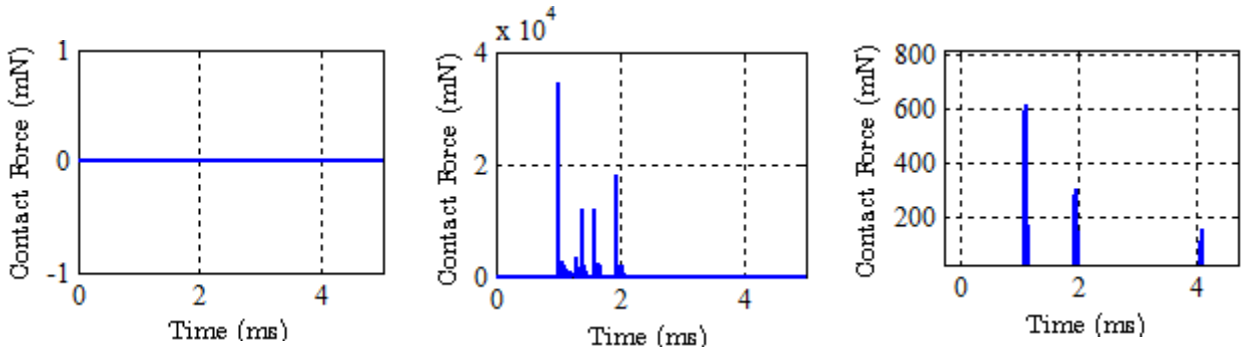

(1) (2) (3)

Fig.6 Disk-ramp contact forces: (1) no ramp model; (2) rigid ramp model; (3) deformable ramp model

In Fig.7 we plot the disk's outer radius displacement at the ramp and the top ramp displacement for the moveable ramp model. It clearly shows three collisions between the

disk and the top ramp while the disk continues its original movement direction after the collisions.

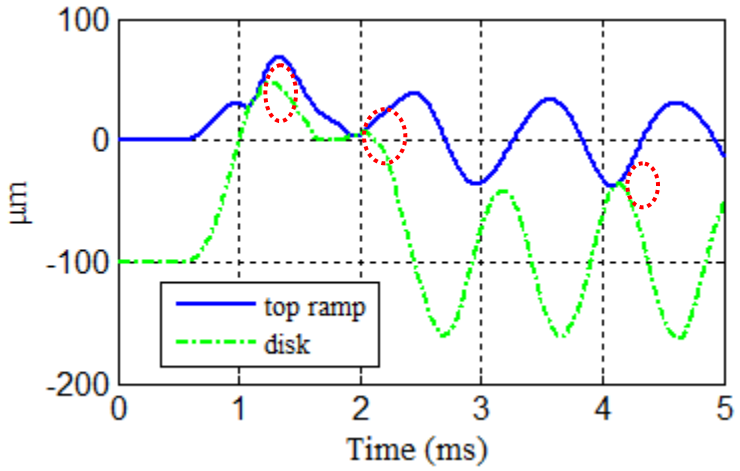

Fig.7 Disk and top ramp displacement at the disk-ramp contact pair position

Fig.8 shows the zoomed-in parts (0.8~1.5 ms) of the disk's (dotted red line) and the slider's (solid blue line) absolute pitches at the slider's center position. Similar to the disk's displacement, the pitches change smoothly in the no-ramp model. In the rigid ramp case, the disk has a relatively large circumferential slope change due to the disk-ramp contacts. The change of the disk's circumferential slope mostly contributes to its pitch in the slider's coordinate system. Therefore, the disk has a sudden pitch change at about 1 ms as shown in Fig.8(2). The solid blue line in Fig.8(2) indicates that the slider's pitch tends to follow the pitch of the disk. However, the suspension's high frequency bending modes are excited during this period (see the oscillations), which may lead to an unstable air bearing. Fig.9(2) presents the minimum clearance between the slider and the disk. It shows that the slider contacts the disk at 1 ms, which may be caused by the air bearing instability. In the deformable ramp case, the disk also has a circumferential slope change (dotted red line in Fig.9(3)), so we can still see the pitch changes for the disk and the slider. Although the slider follows the disk's movement much better in the deformable ramp model than in the

rigid ramp model, the suspension's higher frequency bending modes are excited in this case, as can be seen in Fig.9(3). However, the slider can still fly over the disk successfully.

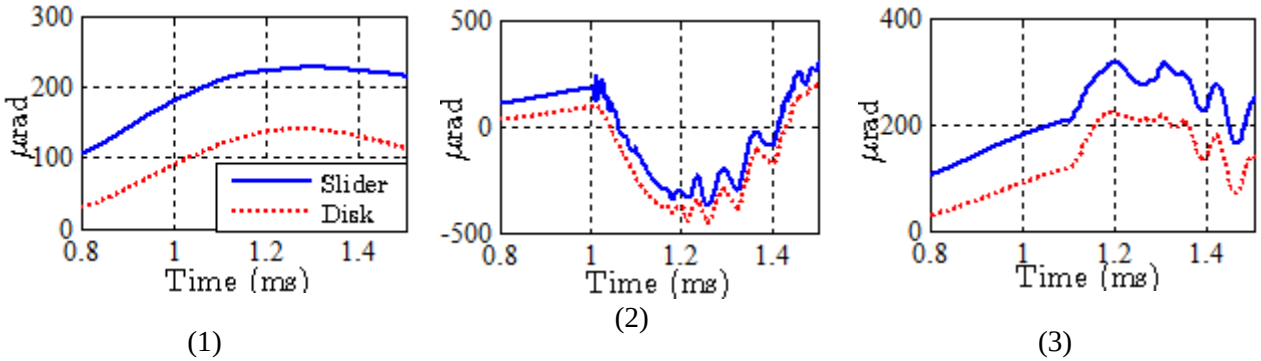

(1) (2) (3)

Fig.8 Disk and slider absolute pitch at slider center position: (1) no ramp model; (2) rigid ramp model; (3) deformable ramp model.

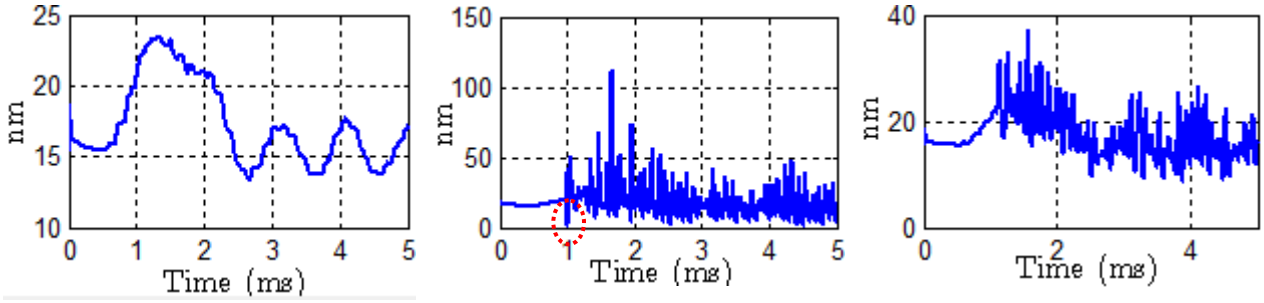

(1) (2) (3)

Fig.9 Minimum clearance between the slider and disk: (1) no ramp model; (2) rigid ramp model; (3) deformable ramp model

From the above comparison of the three models, it appears that the ramps can adversely affect the HDD's working performance during op-shock events. However, the deformable ramp model, which is closer to the actual HDD system, has a safer HDI response than the rigid ramp model.

4.2 Shocks with Pulse Width of 0.5 ms

In this section, an op-shock with shock amplitude of 200G and pulse width of 0.5 ms is applied to the rigid ramp model and the deformable ramp model. Since the excitation frequency is 1 kHz for this shock, which is close to the disk's first mode frequency, the disk's first mode gets excited, and its vibration amplitude is expected to remain almost

constant for some period of time if there is no disk-ramp contact. For the rigid ramp case Fig.10(1) shows that the disk vibrates at an almost constant magnitude and the maximum displacement is slightly less than 50 μm. The contact force shown in Fig.11(1) indicates that the disk contacts the ramps four times. However, the disk-ramp contacts affect the disk's movement only slightly as can be seen in Fig.11(1). That is because the disk's maximum displacement at the ramp position barely exceeds the disk-ramp minimum clearance. Moreover, the slider can fly over the disk successfully, as can be seen in Fig.12(1). However, the structural and HDI responses are quite different for the deformable ramp model. From Fig.10(2), it is observed that the disk's displacement at the slider's center position decays noticeably. Fig.11(2) shows that the disk contacts the top and bottom ramps periodically, and the contact force amplitudes increase as the time increases. This can be explained as follows: because there is a phase difference between the disk's and ramp's movements, the residual vibrations of the disk and ramp increase the disk-ramp contact force, and the increasing disk-ramp contact force again changes the disk's displacement. The severe change of the disk's displacement also affects the slider's flying attitude and causes the slider to crash on the disk as shown in Fig.11(2).

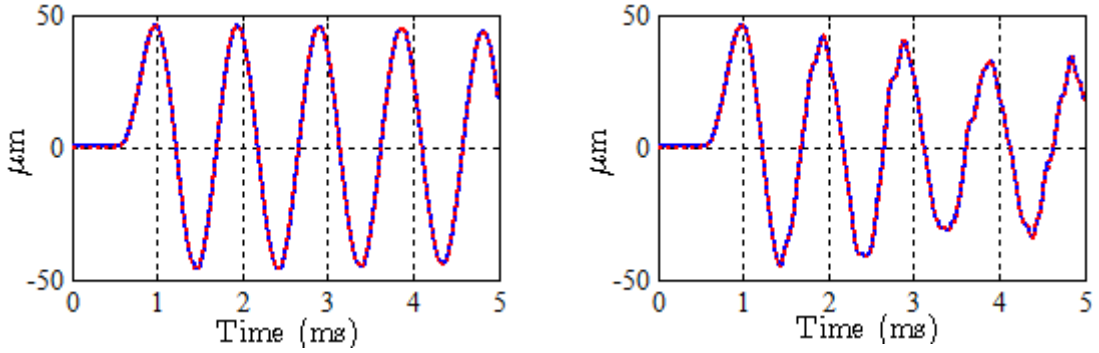

Fig.10 Disk absolute displacement: (1) rigid ramp model; (2) deformable ramp model.

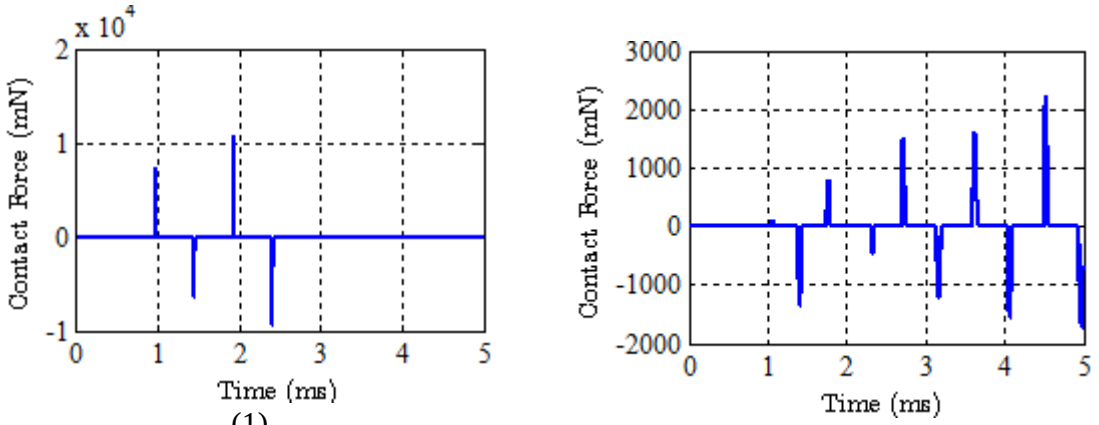

Fig.11 Disk-ramp contact force: (1) rigid ramp model; (2) deformable ramp model.

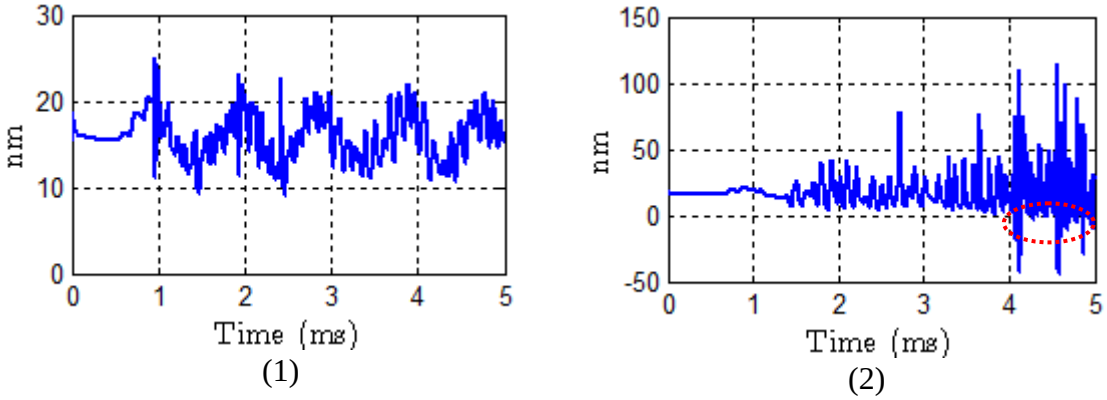

Fig.12 Minimum clearance: (1) rigid ramp model; (2) deformable ramp model.

4.3 Ramp Effects on the Critical Shocks

Critical shock is used as a measure for determining the reliability of a mobile disk drive. It is defined as the maximum shock before the air bearing system fails. Fig.13 plots the critical shock amplitude as a function of shock pulse width for the three ramp models. The critical shock amplitude increases with the increase of pulse width for all three models indicating that the HDD is more easily damaged when it is dropped on a hard floor, which corresponds to a short pulse width. However, the positive and negative critical shock amplitudes are very close to each other in the two ramp models. That is because we consider both top and bottom ramps in the ramp models, and the disk has equal possibility to contact the top and bottom ramps during a positive or negative shock. It is also found

that the deformable ramp model, which is closer to a real HDD, has larger critical shocks than the rigid ramp model, except when the pulse width is small, as explained in section 4.2.

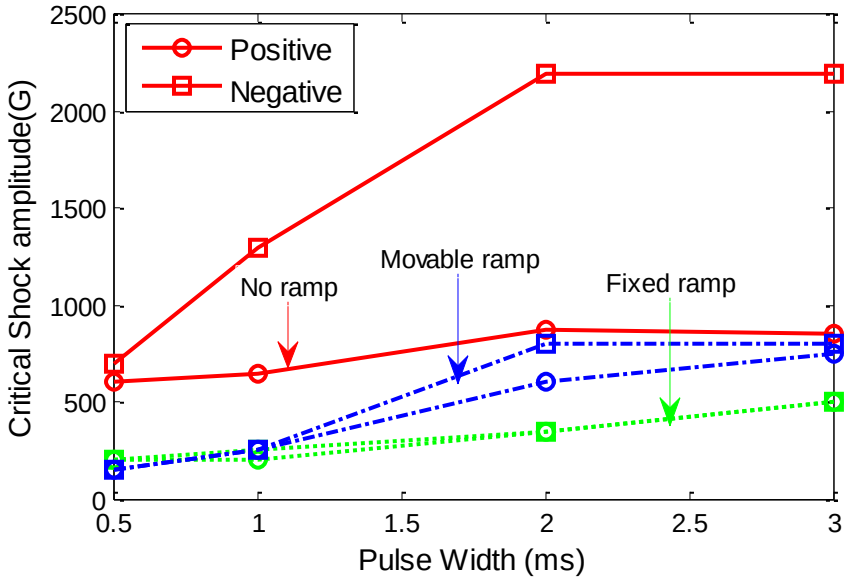

Fig.13 Critical shocks for three ramp models

5. SUMMARY AND CONCLUSION

The deformable ramp constraint has been implemented into the disk op-shock simulation code. The structural and HDI responses are studied in comparison with the previously developed disk op-shock model with a rigid ramp. The slider can more easily crash on the disk in the rigid ramp case when the HDD is subject to a shock with longer pulse widths. When experiencing a shock with short pulse width, the disks and ramps residual vibrations can cause severe disk-ramp contacts or even air bearing instabilities in the deformable ramp case. .

The critical shock is a very essential criterion for indicating the robustness of an air bearing system. The critical shock study for the three ramp models shows that the critical shock amplitude increases with the increase of pulse width for all three models, which

agrees with intuition that the HDD is more easily damaged when it is dropped on a hard floor. Different from the no-ramp model, the positive and negative critical shock amplitudes are very close to each other when the ramps are included in the simulations. However, the deformable ramp model, which is closer to a real HDD, has larger critical shocks than the rigid ramp model, except when the pulse width is small.

REFERENCES

[1] Hitachi. Ramp Load/Unload Technology in Hard Disk Drives. http://www.hgst.com/tech/techlib.nsf/techdocs/9076679E3EE4003E86256FAB005825FB/$file/LoadUnload_white_paper_FINAL.pdf, 2007c.

[2] S. Kumar, V. D. Khanna, M. Sri-Jayantha, "A study of the head disk interface shock failure mechanism," *IEEE Trans. Magn.*, vol. 30(6), pp. 4155–4157, 1994.

[3] T. Kouhei, T. Yamada, Y. Keroba, K. Aruga, "A study of head-disk interface shock resistance," *IEEE Trans. Magn.s,* vol. 31(6), pp. 3006–3008, 1995.

[4] A. M. Allen, D. B. Bogy, "Effects of shock on the head-disk interface," *IEEE Trans. Magn.*, vol. 32(5), pp. 3717–3719, 1996.

[5] J. R. Edwards, "Finite element analysis of the shock response and head slap behavior of a hard disk drive," *IEEE Trans. Magn.,* vol. 35(2), pp. 863–867, 1999.

[6] J. C. Harrison, M. D. Mundt, "Flying height response to mechanical shock during operation of a magnetic hard disk drive," *ASME J. Tribol.,* vol. 122(1), pp. 260–263, 2000.

[7] E. M. Jayson, J. M. Murphy, P. W. Smith, and F. E. Talke, "Shock and Head Slap Simulations of Operational and Nonoperational Hard Disk Drives," *IEEE Trans. Magn.,* vol. 38(5), pp. 2150–2152, 2002.

[8] Q. Zeng and D. B. Bogy, "Numerical Simulation of Shock Response of Disk-Suspension-Slider Air Bearing Systems in Hard Disk Drives," *Microsyst. Technol.,* vol.8, pp. 289-296, 2002.

[9] E. M. Jayson, P. W. Smith, and F. E. Talke, "Shock modeling of the head– media interface in an operational hard disk drive," *IEEE Trans. Magn.,* vol. 39(5), pp. 2429–2431, 2003.

[10] A. N. Murthy, M. Pfabe, J. Xu, F. Talke, "Dynamic response of 1-in. form factor disk drives to external shock and vibration loads," *Microsyst. Technol.,* vol.13, pp. 1031–1038, 2006.

[11] F. Yap, H. Harmoko, M. Liu, N. Vahdati, "Modeling of hard disk drives for shock and vibration analysis-consideration of nonlinearities and discontinuities,", *Nonlinear Dyn.,* vol.50, pp. 717–731, 2007.

[12] M. Liu, F. F. Yap, H. Harmoko, "Shock response analysis of hard disk drive using flexible multibody dynamics formulation," *Microsyst. Technol.,* vol.13, pp. 1039-1045, 2007.

[13] M. Liu, F. F. Yap, H. Harmoko, "A model for a hard disk drive for vibration and shock analysis," *IEEE Trans. Magn.,* vol.44(12), pp. 4764–4768, 2008.

[14] P. Bhargava and D. B. Bogy, "Numerical simulation of operational-shock in small form factor hard disk drives," *ASME J. Tribol.,* vol. 129, pp. 153–160, 2007.

[15] R. Rai, and D. B. Bogy, “Effect of disk support system dynamics on the stability of head–disk interface during an operational shock in a mobile hard disk drive”, Microsyst. Technol., vol.18, pp. 1669-1675, 2012.

[16] R. Rai, and D. B. Bogy, “Parametric study of operational shock in mobile disk drives with disk–ramp contact,” IEEE Trans. Magn., vol 47(7), pp. 1878-1881, 2011.

[17] L. Li, and D. B. Bogy, “Multi-body Modeling Effets on the Head-disk Interface during Operational Shocks in Hard Disk Drives,” 23rd *ASME Annual Conference on Information Storage & Processing Systems*, June 24-25, 2013, Santa Clara, CA.